Journal of The Electrochemical Society, **158** (12) A1483-A1489 (2011)
0013-4651/2011/158(12)/A1483/7/$28.00 © The Electrochemical Society

Mesoporous β-MnO_2 Air Electrode Modified with Pd for Rechargeability in Lithium-Air Battery

Arjun Kumar Thapa, Yuiko Hidaka, Hidehisa Hagiwara, Shintaro Ida, and Tatsumi Ishihara*,z

Department of Applied Chemistry, Faculty of Engineering, Kyushu University, Fukuoka 819-0395, Japan

The electrochemical performance and electrode reactions using ordered mesoporous β-MnO_2 modified with Pd as a cathode catalyst for rechargeable Li-air batteries was reported. Well-ordered mesoporous β-MnO_2 was prepared using mesoporous silica KIT-6 as a template under hydrothermal synthesis of $Mn(NO_3)_2 \cdot H_2O$. The obtained mesoporous β-MnO_2 shows narrow pore size distribution of 1 nm. With the dispersion of small amounts of Pd to β-MnO_2, mesoporous β-MnO_2 exhibited a high initial discharge capacity of 817 mAh/$g_{-cat.}$ with high reversible capacity. Charging potential is suppressed at 3.6 V vs. Li/Li^+, which is highly effective for preventing the decomposition of organic electrolyte. The mesoporous β-MnO_2/Pd electrode shows good rate capability and cycle stability. *Ex-situ* and *in-situ* XRD results suggested that the observed capacity comes primarily from the oxidation of Li^+ to Li_2O_2 followed by Li_2O after discharge to 2.0 V vs. Li/Li^+. Electron spin resonance measurements suggest that the formation of superoxide anion radicals contributs to the oxidation of Li^+ and the radicals were recovered during charge. *Ex-situ* FTIR measurement suggested that no electrolyte decomposition was observed and no Li_2CO_3 was formed during discharge when ethylene carbonate (EC)-diethyl carbonate (DEC) (3:7), which is highly stable for Li-air battery, was used as the electrolyte.
 [DOI: 10.1149/2.090112jes]

Manuscript submitted July 25, 2011; revised manuscript received September 19, 2011. Published November 14, 2011. This was Paper 1011 presented at the Las Vegas, Nevada, Meeting of the Society, October 10–15, 2010.

The coming new energy economy must be based on a cheap and sustainable energy supply. Combined with sustainable resources such as wind and solar power, chemical energy storage using batteries can contribute to a potential solution. Currently, battery research and development is focused on energy storage and conversion with high-energy high-power density and reliable safety.[1–4] Metal-air batteries have attracted considerable attention because of their extremely large specific capacity. The reason for such a large specific capacity is that these cells consist of lithium metal as an anode and an air electrode for activation of oxygen in air; hence these metal-air batteries have a simple structure. Among the various metal-air battery systems, the lithium-air battery is the most attractive because it has the highest energy density per unit weight. The cell discharge reaction occurs between Li and oxygen to yield Li_2O or Li_2O_2, with a theoretical discharge voltage of ca. 3.0 V and a theoretical specific energy density up to 5200 Wh/kg_{-Li}. In practice, the storage of oxygen in the battery is unnecessary, because air can be directly used. Therefore, the theoretical specific energy (excluding oxygen) is 11.140 kWh/kg_{-Li}, which is much higher than that of other advanced batteries and methanol direct fuel cells. Abraham and Jiang reported an Li-air battery using a nonaqueous electrolyte.[5] They suggested that lithium peroxide is a discharge product based on $2(Li^+ + e^-) + O_2 \rightarrow Li_2O_2$, which resulted in a theoretical voltage of 2.96 V. However, because of low oxygen solubility in a nonaqueous electrolyte, the reported power density of an Li-air battery using a nonaqueous electrolyte is much lower than the theoretical value.[6,7] Dobley et al. and Kuboki et al. employed liquid organic solvents as the electrolyte.[8,9] When employing an organic or ionic liquid-based electrolyte solution, the cell reaction produces insoluble Li_2O or Li_2O_2, which precipitates in the pores of the porous carbon-based air electrode to block the further intake of oxygen, abruptly terminating the discharge reaction. Recently, a lithium-air rechargeable battery employing MnO_2 as an air electrode was reported.[10,11] In 2006, Bruce et al. reported that a rechargeable Li–O_2 battery using a carbonate-based electrolyte containing Super S carbon with electrolytic MnO_2 as the catalyst had an initial discharge capacity of 1000 mAh/g (based on the weight of carbon) at a current rate of 70 mA/g and a capacity retention rate of 60% after 50 cycles.[12] Recently, Mizuno et al. also reported that a rechargeable Li–O_2 battery using propylene carbonate (PC) electrolyte containing Ketjenblack (EC600JD) carbon with MnO_2 as the catalyst had an initial discharge capacity of 820 mAh/$g_{-cat.}$ and a capacity retention rate of 60% after 100 cycles, which is the longest cycle life reported for a rechargeable Li–O_2 to date.[13] However, decrease in the charge potential is required because of low energy efficiency for charge and discharge (62% of the reported cell) and also leads to the decomposition of electrolyte resulting in the formation of Li_2CO_3.[14] For this purpose, further improvement in the catalytic activity of an air electrode, one is larger discharge capacity and another is decreased charge potential, is required. MnO_2 can be used as an alternative low cost electrocatalyst for oxygen reduction/evolution reactions.[15] However, MnO_2 prepared by the traditional ceramic route has limited electrocatalytic activity because of its large particle size and low specific surface area.[16] In addition, decomposition of electrolytes containing propylene carbonate (PC) leads to the formation of Li_2CO_3; this is the main reason for the high charge potential.[13] Previously, we studied mesoporous α-MnO_2 modified with a Pd cathode air electrode for a rechargeable Li-air battery, which showed higher reversible capacity as well as higher current density than the standard Li-air battery.[17] In the current study, we synthesized mesoporous β-MnO_2 using silica KIT-6 as a template and applied it as a cathode catalyst for an Li-air battery. We found that a mixture of Pd and mesoporous β-MnO_2 shows high oxidation activity and Li^+ undergoes reduction to form Li_2O_2 or Li_2O, even in a dry atmosphere. We also pointed out negligible decomposition of organic electrolyte by decreasing the charge potentials and using the stable electrolyte.

Experimental

Sample preparation.— Mesoporous β-MnO_2 was prepared using mesoporous silica KIT-6 as a template. The mesoporous silica KIT-6 template was prepared in according with the literature.[18,19] $Mn(NO_3)_2 \cdot 6H_2O$ (3 g) was dissolved in ethanol (15 ml) and then the mesoporous silica KIT-6 template was added in a beaker. The mixture was stirred continuously at room temperature till all of the solution was adsorbed. The solid product was then heated slowly to 573 K for 3 h and allowed to cool slowly. The product was reheated to 623 K at the rate of 1 K/min for 5 h. Mesoporous β-MnO_2 was treated with hot 2M NaOH solution to remove the silica KIT template and then washed with distilled water and ethanol several times. The product was then kept at 333 K for 12 h to remove the moisture.

Measurement of air electrode performance for Li-air battery.— The electrochemical characterizations were carried out using a

* Electrochemical Society Active Member.
z E-mail: ishihara@cstf.kyushu-u.ac.jp

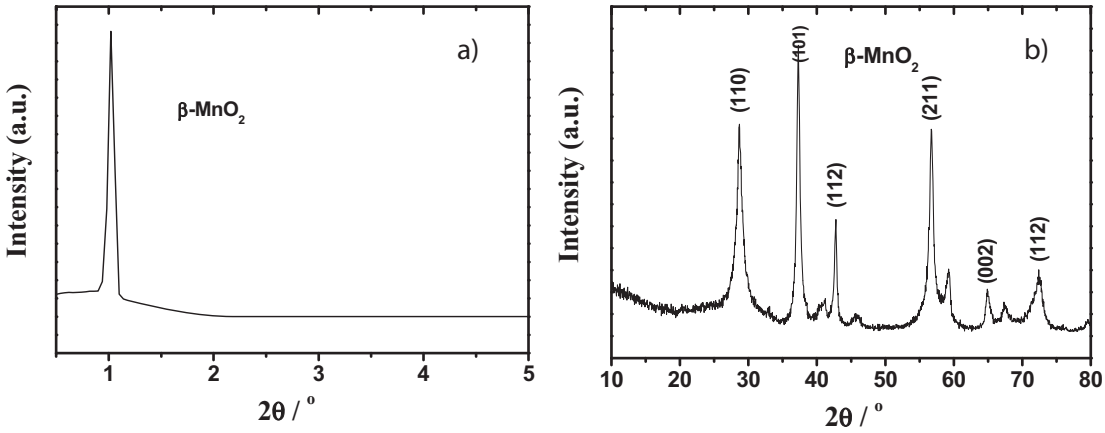

Figure 1. (a) Low-angle and (b) wide-angle XRD patterns of mesoporous β-MnO_2.

Swagelok-type cell. The cathode was formed by casting a mixture of mesoporous β-MnO_2, PdO, and PTFE-coated teflonized acetylene black (TAB-2) as a conducting binder (mol ratio of 75:15:10). The resulting mixture was pressed onto a stainless steel mesh and the cathode was dried at 433 K for 12 h under vacuum. It is also noted that PdO in air electrode was reduced to Pd during first charge because only X-ray diffraction peak assigned to metallic Pd was observed.

Li-air cell measurements were carried out at room temperature. The Li-air battery configuration used in this study consists of a lithium foil (12 mm in diameter) as an anode electrode separated by two pieces of porous polypropylene film (Celgard 3401). The cell was gas tight except for the stainless steel mesh window that exposed the porous cathode to O_2 atmosphere. The electrolyte used was 1M lithium bis(trifluoromethanesulfonyl)imide-ethylene carbonate:diethyl carbonate (LiTFSI-EC:DEC, 3:7 by volume) supplied by Ube Chemical Co. Ltd. Charge–discharge performance was carried out at a voltage range of 4.0–2.0 V at current densities of 0.025–5.1 mA cm^{-2}. In this study, for capacity comparison, we normalized the observed capacity by the total weight of the air electrode, not by the weight of carbon. A practical lithium-air battery should be tested under ambient conditions. The moisture content in the air reacts with the lithium negative electrode and CO_2 consumes all the lithium salt in the electrolyte. To avoid such negative effects, the cell was tested in a pure dry oxygen atmosphere.

Characterization.— Powder X-ray diffraction (XRD) analysis of mesoporous β-MnO_2 was carried out with CuKα radiation (λ = 1.541 Å, Rigaku Rint 2500) at the low-angle scanning range of 0.5–5° and a wide-angle range of 10–80° (2θ) with a scan speed of 0.02°/s. *In-situ* XRD measurement during discharge and charge was performed in this study. The commercial *in-situ* XRD measurement cell (Rigaku) was used in this study. The cell consists of a polyimide film window with an open hole. An air electrode of 0.2 g and metal Li were set in the XRD measurement cell. The *in-situ* cell was put into a polyethylene bag and oxygen was substituted for the atmosphere. A current density of 0.02 mA/cm^2 was applied, and when the potential reached the target value, the XRD measurement was performed using CuKα line (Rigaku Rint-Mini).

A Keyence VE-7800 was used to obtain a scanning electron microscope image. A JEOL JEM 2100 operated at 200 kV was used to obtain a transmission electron microscope image. Specific surface area (S_{BET}) was determined from nitrogen adsorption–desorption isotherm using Nippon Bell, BELSORP 18PLUS-FS, Japan.

Examination of the discharge electrode involved disassembling the cell in the glove box, rinsing the cathode electrode three times with diethyl carbonate for removing the solvent under vacuum, and then sealing the electrodes in a polyvinyl bag in an argon-filled glove box to prevent any reaction with moisture or CO_2 in the air. Electron spin resonance (ESR) measurement was performed at room temperature using Bruker, type EMK8 to remove the air electrode from the cell and to analyze the oxygen radicals by dilution with silica glass sand. FT-IR measurement was performed with transmission method using KBr windows and mercury cadmium telluride (MCT) semiconductor detector was used. Commercial FT-IR spectrometer (Type 610, JASCO co ltd.) was used and the samples was mounted in the gastight IR cell after charge and discharge measurement.

Results and Discussion

Structure and morphology of prepared β-MnO_2.— Figure 1a illustrates the low-angle XRD patterns of mesoporous β-MnO_2. A sharp diffraction intensity peak was observed at 1.02°, suggesting the formation of a mesoporous structure. The estimated diameter of the mesopores in β-MnO_2 was 0.85 nm, which corresponds to the inner diameter of mesoporous β-MnO_2. From the XRD pattern, it was confirmed that mesoporous β-MnO_2 was successfully synthesized by a hydrothermal synthesis process. Figure 1b shows the wide-angle XRD pattern of the prepared samples, and it was confirmed that all diffraction peaks could be assigned to the mesoporous β-MnO_2 phase. Because no diffraction peaks from an impurity phase were observed in the wide-angle XRD pattern, it can be reasonably concluded that a single β-MnO_2 phase with a mesoporous structure was successfully prepared. From the XRD database (JCPDS No. # 24-0735), the prepared sample could be assigned to a tetragonal lattice of β-MnO_2 [space group P42/*mnm*], where the lattice parameter values are a = 4.404 Å, b = 4.404 Å, and c = 2.876 Å.

Figure 2a shows the scanning electron microscope images of mesoporous β-MnO_2 in which small microparticles of 0.1–0.3 μm

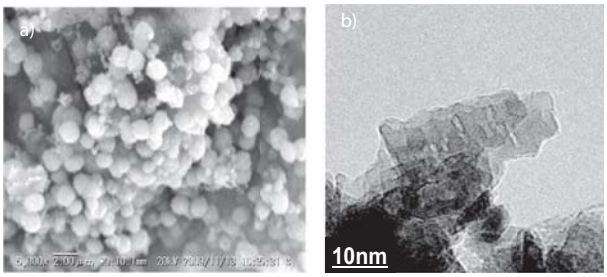

Figure 2. (a) SEM image of mesoporous β-MnO_2 and (b) TEM image of mesoporous β-MnO_2.

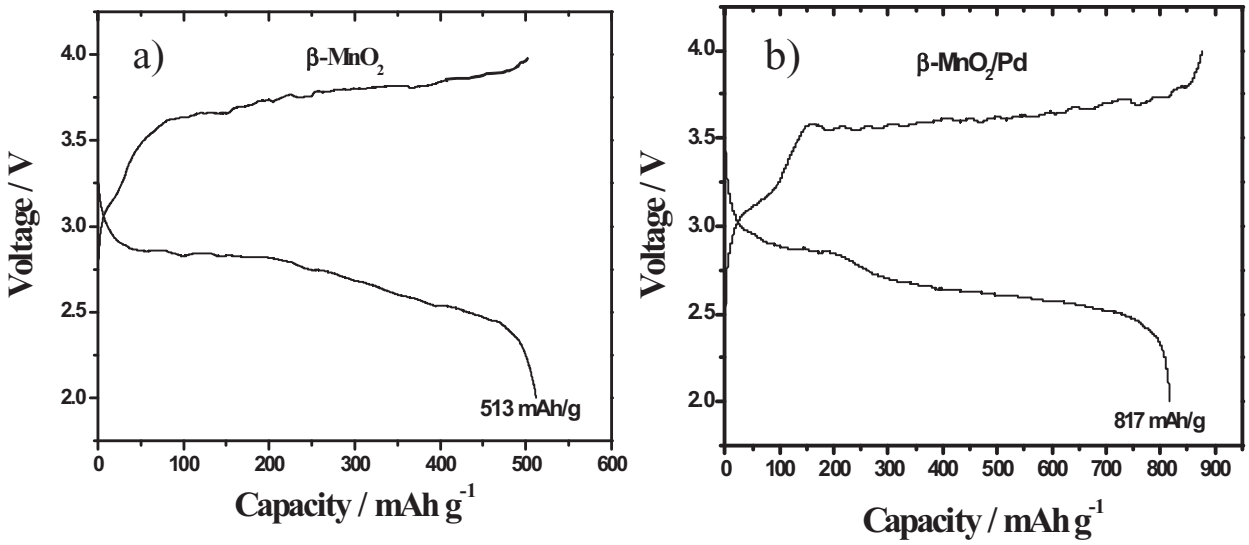

Figure 3. Charge–discharge curves of lithium-air battery using mesoporous (a) β-MnO_2 and (b) Pd/β-MnO_2 air electrode in an O_2 atmosphere between 4.0–2.0 V at a current density of 0.025 mA cm^{-2}.

diameter were aggregated to form large spherical secondary particles of ca. 1 μm diameter. The TEM image of mesoporous β-MnO_2 shown in Figure 2b indicates many pores with no regular structure. Therefore, the pore structure seems to be the so-called wormhole-like pore structure. The estimated size of the pore from the TEM observation was ca. 1 nm, which agrees closely with that estimated from the low-angle diffraction peak (0.8 nm). N_2 adsorption–desorption isotherm curves of mesoporous β-MnO_2 were also studied. Mesoporous β-MnO_2 showed a typical type IV curve with H_1 hysteresis loop, which is characteristic of a typical mesopore structure. S_{BET} of mesoporous β-MnO_2 was 29.0 m^2 g^{-1}. The pore size distribution of mesoporous β-MnO_2 was 4.0–6.1 nm with a pore volume of 0.38 cm^3 g^{-1}. The observed pore seems to be space between particles but not mesopores.

Charge–discharge property of Pd/mesoporous β-MnO_2.— The electrocatalytic activities of β-MnO_2/TAB-2 (90:10) and β-MnO_2/Pd/TAB-2 (75/15/10) air electrode in the Li-air battery were measured. Although propylene carbonate based electrolyte was widely used for organic electrolyte of Li-air battery, we used 1M lithium bis(trifluoromethanesulfonyl)imide-ethylene carbonate:diethyl carbonate (LiTFSI-EC:DEC, 3:7 by volume) for electrolyte because of high chemical stability. However, in order to prevent decomposition, applied potential should be lower than 4 V. Figure 3 shows the charge–discharge curve of the Li-air cell. Mesoporous β-MnO_2 had an initial discharge capacity of ca. 513 mAh $g_{-cat.}{}^{-1}$ during the first cycle (Figure 3a). The discharge plateau curve was large and flat at 2.8–2.9 V, which is comparable to reported data.[11] However, the charge potential plateau curve was observed at 3.7 V, which is slightly higher than the theoretical potential of 2.95 V vs. Li/Li^+. In our previous study, we found that Pd was highly active for Li^+ oxidation and decomposition of Li_2O_2 or Li_2O.[16,17] Loading of Pd on MnO_2 shows high energy efficiency for charge and discharge; hence, loading of Pd on mesoporous β-MnO_2 was further studied. The addition of a small amount of Pd to the mesoporous β-MnO_2 increased the capacity to ca. 817 mAh $g_{-cat.}{}^{-1}$, as shown in Figure 3b. With the dispersion of a small amount of Pd to β-MnO_2, the discharge potential plateau curve also shifted toward the high potential of 2.9 V vs. Li/Li^+, which is close to the theoretical value of 2.95 V vs. Li/Li^+ for Li_2O_2 formation. Increase in discharge potential is simply explained by the decreased electrode over potential by loading of the active Pd catalyst. The charge potential was also suppressed at 3.6 V vs. Li/Li^+ and showed a large and flat plateau curve with high reversible capacity. The above charge–discharge curve of mesoporous β-MnO_2 electrode with added Pd for the Li-air battery shows that the efficiency of charge and discharge increased drastically from 65% to 77.8%.

The rate property of Li-air is generally not good; however, if the air catalyst is highly active, then a reasonably high rate property is expected. In this study, the charge and discharge rate properties of the cell were also studied using the mesoporous β-MnO_2/Pd air electrode. The charge–discharge curve of the cell is shown in Figure 4 at various current densities. By applying a current density of 0.025 mA cm^{-2}, the mesoporous β-MnO_2/Pd electrode showed a discharge capacity of 817 mAh $g_{-cat.}{}^{-1}$. The charge capacity decreased as the current density increased; however, it was found that for a current density as high as 5.1 mA cm^{-2}, the β-MnO_2/Pd electrode still retained the discharge capacity of 93 mAh $g_{-cat.}{}^{-1}$, which is 11.3% of its initial capacity. The mesoporous β-MnO_2/Pd electrode showed high capacity comparable to current lithium-ion batteries such as those of $LiMn_2O_4$. This indicates that the rate property of the current Li-air battery is reasonably high, which can be attributed to the high activity of the present air electrode. Here the mesoporous β-MnO_2/Pd air electrode showed a large capacity even at high current density. The porocity of the air electrode was not high and slso Li foil with small surface area used for anode. Therefore, one reason for the decreased discharge capacity at high current density might be the slow dissolution rate of Li metal into electrolyte and also slow diffusion of Li^+ in the air electrode to active site. In any case, although the Li-air battery is considered to have a low rate property and shows only large capacity at a low current density, reasonably high capacity was exhibited at high current density for the cell using Pd/mesoporous β-MnO_2.

Cycle stability at low current density is also studied. Figure 5 shows the capacity as a function of cycle number of the mesoporous β-MnO_2/Pd air cathode electrode at low and high current densities. The mesoporous β-MnO_2/Pd electrode showed an initial discharge capacity of 578 mAh $g_{-cat.}{}^{-1}$ during the initial cycle. After 13 cycles, it retained the capacity of 417 mAh $g_{-cat.}{}^{-1}$ at 0.12 mA cm^{-2}. At high current densities, it showed an initial discharge capacity of 208 mAh $g_{-cat.}{}^{-1}$ at 1.91 mA cm^{-2} during the initial cycle. After 13 cycles, it retained the capacity of 134 mAh $g_{-cat.}{}^{-1}$ at 1.91 mA cm^{-2}. The capacity retention rates of the β-MnO_2/Pd electrode at low and high current densities were 72.2% and 64.9%, respectively, after 13 cycles, which is much higher than the renention rate reported by other groups.[10,11,13] Therefore, the cycle stability of the cell is reasonably high and the Li-air cell can be used as a rechargeable battery.

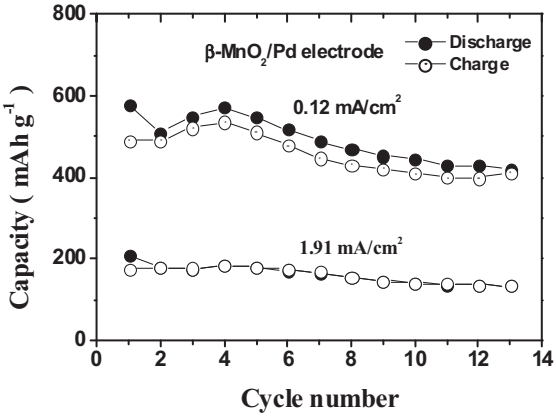

Figure 4. Charge–discharge capacities versus cycle performance of mesoporous β-MnO_2/Pd/TAB (75/15/10) electrode at current densities of 0.12 and 1.91 mA cm^{-2}.

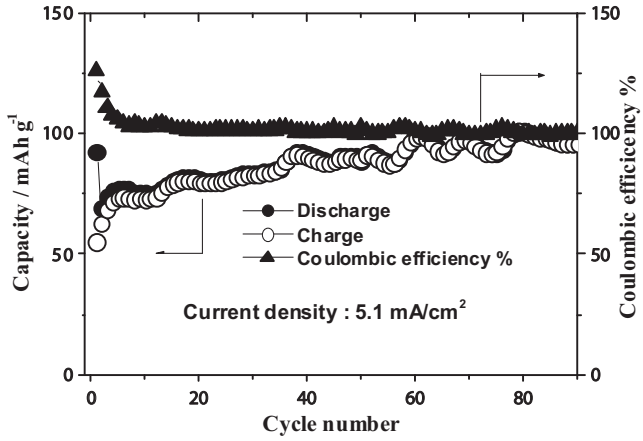

Figure 6. Charge discharge capacities versus cycle numbers of the Li-air cell using mesoporous β-MnO_2/Pd/TAB (75/15/10) air electrode at current density of 5.1 mA cm^{-2}.

Further longer cycle stability was studied at higher current density, 5.1 mA cm^{-2}. Figure 6 shows the capacity as a function of cycle number of the mesoporous β-MnO_2/Pd air cathode electrode at the current density of 5.1 mA cm^{-2}. The mesoporous β-MnO_2/Pd air electrode showed an initial discharge capacity of 93 mAh $g_{-cat.}{}^{-1}$ during the initial cycle. The charge–discharge measurement showed a decrease in discharge capacity during the second cycle. However, further charge-discharge measurement showed a gradual increase in capacity of up to 95 mAh $g_{-cat.}{}^{-1}$ during the 92nd cycles. After the 93rd cycle, capacity fading was observed owing to increase in internal resistance of the cell caused by evaporation of the carbonate electrolyte. This is the first study to report that Li-air battery can be rechargeable even at a current density as high as 5.1 mA cm^{-2} for up to ca. 100 cycles.

The *ex-situ* XRD of the β-MnO_2/Pd electrodes before charge and after discharge to 200 mAh $g_{-cat.}{}^{-1}$, 400 mAh $g_{-cat.}{}^{-1}$, and 2.0 V vs. Li/Li^+, respectively, were measured in this study, because two potential plateaus were observed for discharge in the Li-air battery. Figure 7 shows the *ex-situ* XRD results of the β-MnO_2/Pd electrodes before charge and after discharge. After discharge to 200 mAh $g_{-cat.}{}^{-1}$, the mesoporous β-MnO_2/Pd electrode showed a new peak at 52°, which corresponds to the stainless steel (SUS) mesh. After discharge to 400 mAh $g_{-cat.}{}^{-1}$, the *ex-situ* XRD of the β-MnO_2/Pd electrode showed a peak at 23°, which was assigned to the peak from the polythene bag. At 35° another new peak started to appear that could be assigned to the formation of Li_2O_2. After discharge to 2.0 V, the broad peak at 35° was retained. In addition to the peak at 35°, new broad peaks, which are assigned to the peak from Li_2O, were also observed at ca. 34 and 66°. These results suggest that Li_2O_2 forms at the initial highpotential range as well as at the low potential range of 2.0 V. In contrast, the strong peak of Li_2O at 2.0 V suggests that Li_2O is also formed during discharge, in particular, at the low potential range. It has been reported by several groups that Li_2O_2 is the main product in Li-air batteries; however, this study confirmed that Li_2O is also formed during discharge. In addition, as illustrated in Figure 7, it is evident that no peaks were assigned to Li_2CO_3, which is another possible product during discharge of the Li-air battery. In our previous study, we found that low carbon content in an air electrode effectively prevents Li_2CO_3 formation and results in low discharge potential. Therefore, in this study, the low discharge potential of the cell using the β-MnO_2/Pd air electrode can be explained by the absence of Li_2CO_3 formation. It is also noted that Li_2O was formed when Pd was used as the air electrode. This could be explained by the high activity of Pd for the dissociation of the oxygen–oxygen (O-O) bond.

The discharge products of the air electrode were further studied with Raman spectroscopy. Raman spectroscopic analysis is reported to be highly sensitive to Li_2O and Li_2O_2. As shown in Figure 8, characteristic Raman peaks for Li_2O and Li_2O_2 were observed after discharge at 250 and 500 cm^{-1}, respectively. Because the peak intensity of Li_2O was much stronger than that of Li_2O_2, the Raman spectra suggest that the main product in β-MnO_2/Pd was Li_2O after

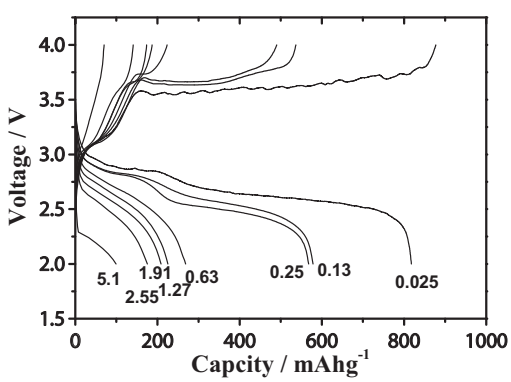

Figure 5. First charge–discharge curves of the cell using mesoporous β-MnO_2/Pd/TAB (75/15/10) air electrode at different current densities. Number in figure means currdent density for charge and discharge (mA/cm^2).

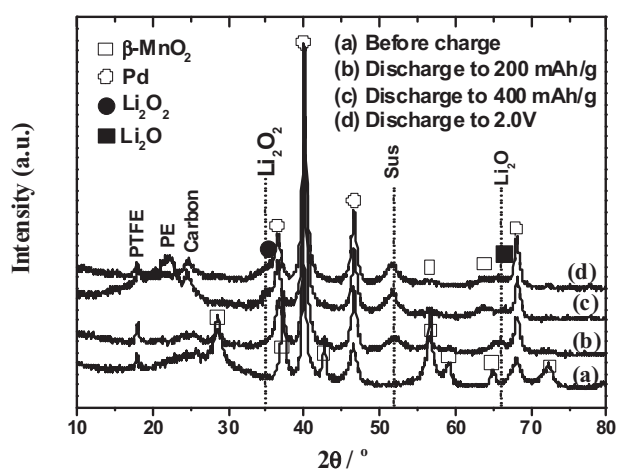

Figure 7. *Ex-situ* XRD of mesoporous β-MnO_2/Pd/TAB (75/15/10) electrode before discharge and after discharge to 200 and 400 mAh $g_{-cat.}{}^{-1}$ at 2.0 V.

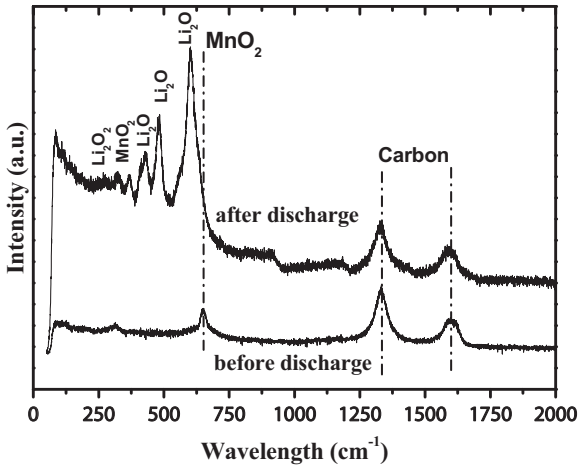

Figure 8. *Ex-situ* Raman spectroscopy of mesoporous β-MnO_2/Pd/TAB (75/15/10) electrode before discharge and after discharge to 2.0 V.

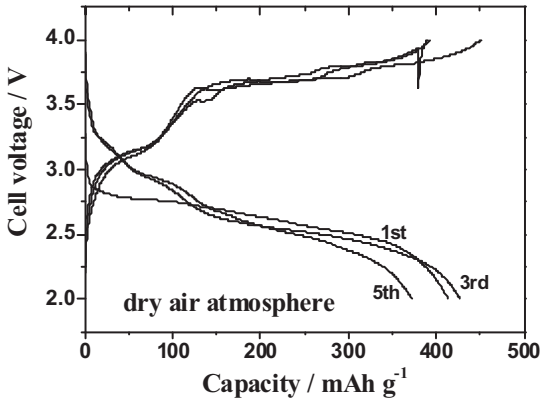

Figure 9. Charge–discharge curves of a lithium-air battery using mesoporous β-MnO_2 modified with Pd air electrode in dry air atmosphere between 4.0–2.0 V at a current density of 0.12 mA cm^{-2}.

discharge to 2.0 V. Many studies have reported Li_2O_2 as the main discharge product[11,12] and small Li_2O formation amount after discharge. Furthermore, in this study, we observed Li_2O as the main discharge product. This difference could be explained by the activity of the air electrode in relation to the dissociation of the O-O bond, which will be discussed in detail later in this paper. In contrast, no Li_2CO_3 peaks were observed at 1090 cm^{-1} in the Raman spectra after discharge, which suggests that Li_2CO_3 was not formed. Therefore, both Raman spectra and XRD measurements show negligible Li_2CO_3 formation. This could be related to the low charge potential around 3.7 V and the small amount of carbon binder used for the air electrode. It has also been reported that significant decomposition of carbonate electrolytes, in particular, propylene carbonate (PC), occurs at a potential higher than 4.0 V.[13,20,21]

The effect of air instead of O_2 was further studied. It was found that the discharge capacity increased monotonously as the oxygen partial pressure increased. Therefore, it is reasonable to conclude that a high oxygen partial pressure is suitable for achieving a high capacity. However, to date, the application of real air has not been studied in detail. Compared with the discharge in O_2, the potential plateau and the discharge capacity both decreased slightly in dry air (Fig. 9). However, decrease in capacity was not large; a fairly large discharge capacity of ca. 417 mAh $g_{\text{-cat.}}^{-1}$ was observed. In contrast, the charge potential increased to 3.6 V vs. Li/Li^+ when dry air was substituted for O_2. XRD measurement after discharge in dry air also suggests that no Li_2CO_3 diffraction peaks was observed.

Charge and discharge mechanism on β-MnO_2/Pd.— The charge–discharge mechanism of the Li-air battery is not yet well understood. As shown in Figure 3, two potential plateaus were observed at 2.9 and 2.7 V in the discharge curves and at 3.5 and 3.7 V in the charge curves. This suggests that Li_2O_2 and Li_2O formations were related to charge and discharge in the studied cell. *In-situ* XRD measurements were performed for the Pd/β-MnO_2 air electrode in the Li-air cell by using a homemade cell in substituted atmosphere. Figure 10 shows the *in-situ* XRD patterns of the Pd/β-MnO_2 air electrode during discharge. Before discharge, it is obvious that all diffraction peaks can be assigned to Pd and β-MnO_2. With decreasing potential, the intensity of the diffraction peaks from Pd and β-MnO_2 increased slightly. This might be explained by the slight change in the height of the sample because insoluble Li_2O_2 and Li_2O products are deposited. At ca. 2.8–2.7 V, diffraction peaks were observed around 34.8 and 49.8° (shoulder peaks of Pd) and

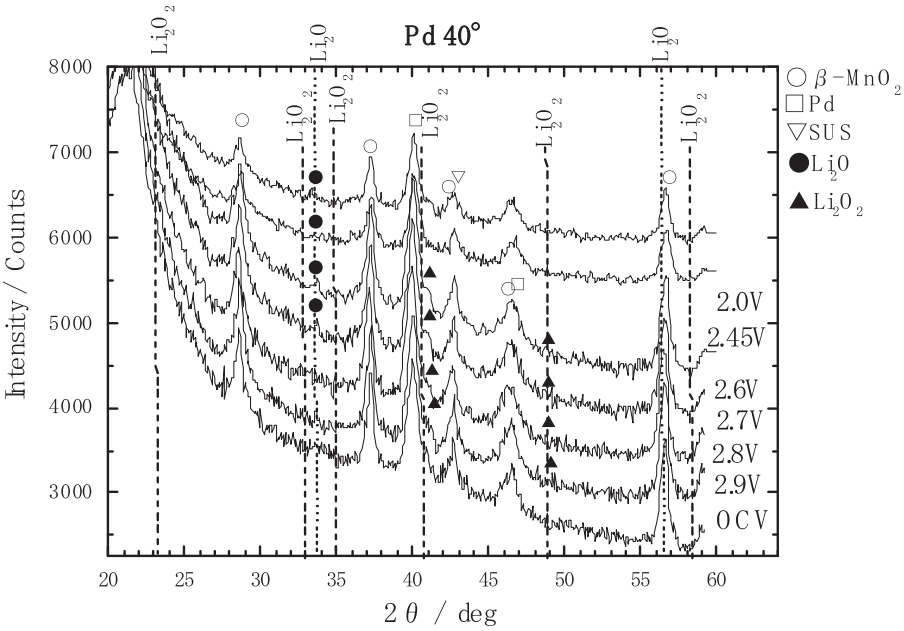

Figure 10. *In-situ* XRD of mesoporous β-MnO_2/Pd/TAB (75/15/10) cathode air electrode for rechargeable Li-air battery during discharge state in open-air atmosphere.

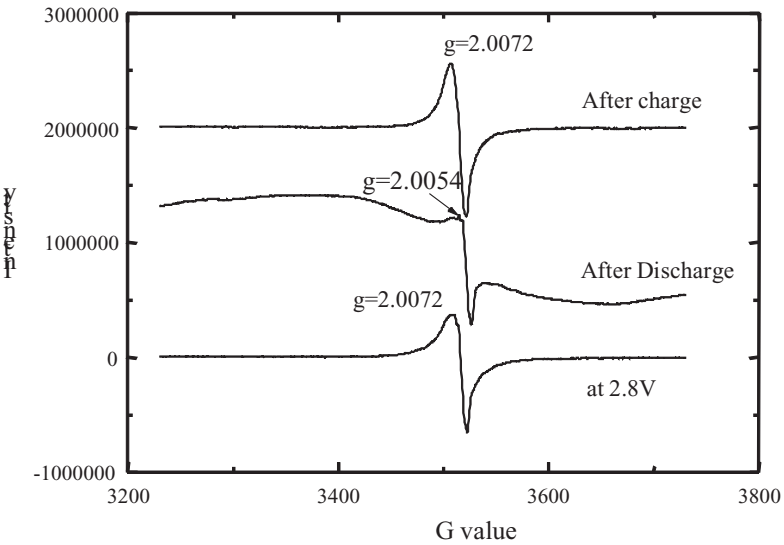

Figure 11. Electron spin resonance (ESR) spectra of Pd/β-MnO_2 during discharge and charge.

these peaks can be attributed to Li_2O_2. As the potential decreased, at around 33.8°, a diffraction peak that can be attributed to Li_2O became significant and the peaks assigned to Li_2O_2 were weakened. Therefore, Li_2O_2 was formed at high potential plateau and followed by Li_2O at low potential. This observation is valid considering the standard potential of Li_2O_2 (2.95 V vs. Li/Li^+) and Li_2O (2.90 V vs. Li/Li^+) for the Li-air battery. Considering the change in weak strength, it is likely that Li_2O formed successively from Li_2O_2.

ESR measurements were also performed on active oxygen species in this study. On the basis of Raman spectroscopy results, Bruce et al. reported that oxygen radical is an active species for oxidation of Li.[21] Figure 11 shows the ESR spectra of the air electrode at 2.8 and 2.0 V for discharge and 4 V for charge. Evidently, two ESR signals at g = 2.007 were observed at the initial discharge process. The ESR signal at g = 2.007 is typical of superoxide anion radicals (O_2^-).[22,23] After discharge, the intensity of this ESR peak decreased drastically, suggesting that O_2^- contributes to the formation of Li_2O_2 or Li_2O. Although we did not detect LiO_2, Bruce et al. reported that the initial product in an air electrode is LiO_2 from the Raman spectra.[21] Considering the ESR and *in-situ* XRD results, the reaction steps for discharge in the present cell seem to be as follows:

$$O_2 + e^- = O_2^-$$

$$O_2^- + Li^+ = LiO_2$$

$$LiO_2 + Li^+ + e^- = Li_2O_2$$

$$Li_2O_2 + 2Li^+ + 2e^- = 2Li_2O$$

According to this reaction mechanism, the Li ion reacts with molecular oxygen. In the final step, the O-O bond fractures to form Li_2O. A similar reaction mechanism is also reported for the formation of H_2O_2 from O_2 and H_2.[24,25] Pd is a well-known catalyst for the fracture of O-O bond.[26] Therefore, Li_2O formation, which has not been reported by other groups, was observed on the examined Pd/β-MnO_2 composite catalyst in this study. It has been reported that superoxide anion radicals form on oxygen vacancy[21] and MnO_2 is easily partially reduced, i.e., Mn^{3+} is easily formed. Therefore, it is expected that mesoporous β-MnO_2 could be an active site for the formation of superoxide anion radicals. The bifunctional roles of MnO_2 and Pd for the formation of superoxide anion radicals and separation of the O-O bond, respectively, are suspected during the discharge process. The similar reaction route was also reported by Laoire et al. [27,28]

During charge, Li_2O might largely decompose at 3.7 V to form Li and oxygen, which might indicate the presence of superoxide anion radicals because the ESR signal was recovered after discharge. Furthermore, a small amount of Li_2O_2 was also observed at the final stage of discharge (down to 2.0 V) as shown in Figs. 3 and 9. Based on the linear potential sweep measurement, decomposition of Li_2O_2 was observed around 3.5 V and of Li_2O at a potential higher than 3.7 V. Therefore, a small potential plateau at 3.5 V during charge can be attributed to the decomposition of Li_2O_2 and a large plateau at a potential higher than 3.7 could indicate the decomposition of Li_2O. However, the charge process requires further detail study.

Further, carbonate-based electrolytes decomposed with oxygen radicals through lithiated organic carbonates to form Li_2CO_3. In this study, changes in electrolytes before and after the charge and discharge cycle were measured with FTIR. Figure 12 shows the FTIR spectra of the pristine Pd/β-MnO_2 electrode after first discharge and then after recharging to 4.0 V in 1M LiTFSI-EC:DEC(3:7) under O_2 atmosphere. Evidently, IR peaks assigned to carbonate were observed; however, no significant change in the IR spectra of EC-DEC (3:7) electrolyte was observed. Mizuno et al. reported that lithium alkyl carbonate absorption peaks at 1650, 1360, and 825 cm^{-1} were formed during charge and discharge.[13] However, no peaks were observed at the frequency shown in Figure 12, suggesting that in this study, no significant electrolyte decomposition occurs. McCloskey et al. reported that electrolyte decomposition is strongly related to the electrolyte compound used.[20] Therefore, the electrolyte of 1M LiTFSI/EC-DEC (3:7) used in this study seems to be reasonably stable when electrochemical windows between 2.0 and 4.0 V are used and when small amounts of carbon are present in the air electrode. This also agrees well with the result that negligible Li_2CO_3 was formed in this study. One reason for negligible Li_2CO_3 formation is that the charge potential was limited to 4.0 V and a small amount of carbon was used as the air electrode. The results from many other groups indicate a large amount of carbon in the air electrode. However, in our previous results, it was found that a MnO_2 electrode with no carbon shows high reversibility without forming Li_2CO_3.[16] In any case, in this study, the organic electrolyte 1M LiTFSI/EC-DEC (3:7) did not decompose significantly during charge and discharge in a electrochemical window from 2 to 4 V vs. Li/Li^+. This is important for reversibility of Li-air battery.

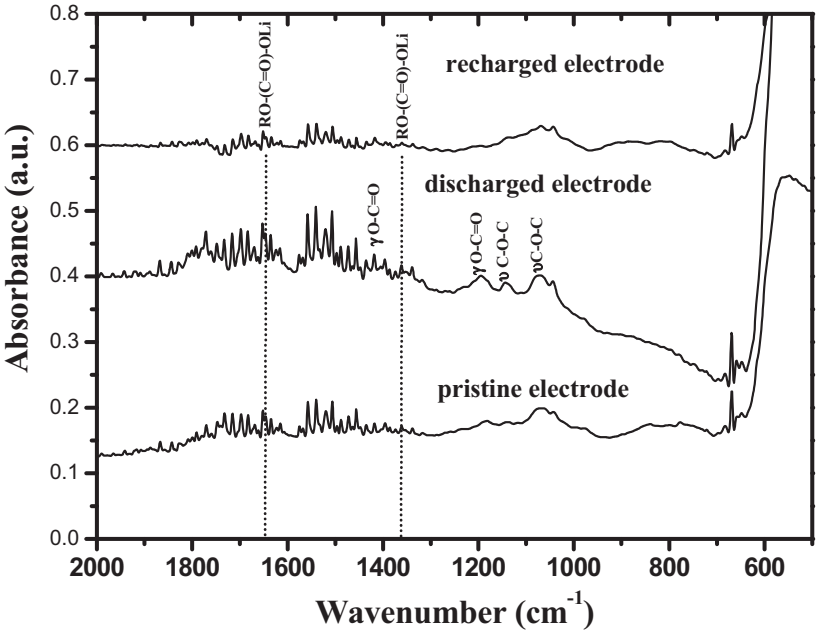

Figure 12. FTIR spectra of Pd/β-MnO_2 pristine electrode after first discharge and then charge in 1M LiTFSI-EC:DEC (3:7) under O_2 atmosphere.

Conclusion

In summary, this study reveals that a mesoporous β-MnO_2/Pd electrode is highly active for a rechargeable Li-air battery and is effective for increasing discharge and decreasing charge potentials. This configuration results in energy efficiency. Even at reasonably high current density, high reversible capacity was achieved in both pure O_2 and dry air atmospheres. These results suggest that lithium-air batteries can be rechargeable even at high current densities. Using the mesoporous β-MnO_2/Pd electrode, *ex-situ* and *in-situ* XRD results show the formation of Li_2O_2 followed by Li_2O after discharge to 2.0 V. The ESR measurements also suggest that superoxide anion radicals contribute to the oxidation of Li ions and during the charge process, superoxide anion radicals are recovered. In this study, energy efficiency of up to 80.5% for charge and discharge were achieved. This is much higher than the reported data to date. This level of energy efficiency can be achieved by the bifunctional activities of Pd/β-MnO_2 for charge and discharge reactions and by the prevention of EC-DEC (3:7) electrolyte decomposition by limiting the amount of carbon binder and charge potential up to 4.0 V. On the other hand, comparing with discharge capacity by using Pd/α-MnO_2 which has molecular size tunnel structure, much larger discharge capacity was observed on Pd/β-MnO_2 in spite of the similar surface area. Measoporous structure of β-MnO_2 is wormhole-like pore and that of α-MnO_2 is straight. Therefore, I think simple straight mesopore is easily blocked with deposited Li oxide and so mesopore with complicated structure seems to be effective for achieving the large capacity in Li-air battery. Consequently, controle of mesopore structure is important for air electrode of a Li-air battery.

Acknowledgments

This study was financially supported by the Li-EAD project of the New Energy and Industrial Technology Development Organization (NEDO) of Japan.

References

1. M. Winter and R. J. Brodd, *Chem. Rev.*, **104**, 4245 (2004).
2. M. Armand and J. M. Tarascon, *Nature*, **451**, 652 (2008).
3. J. Chen and F. Cheng, *Acc. Chem. Res.*, **42**, 713 (2008).
4. J. M. Tarascon and M. Armand, *Nature*, **414**, 359 (2001).
5. K. M. Abraham and Z. Jiang, *J. Electrochem. Soc.*, **143**, 1 (1996).
6. J. Read, *J. Electrochem. Soc.*, **149**, A1190 (2002).
7. J. Read, K. Mutolo, M. Ervin, W. Behl, J. Wolfenstine, A. Driedger, and D. Foster, *J. Electrochem. Soc.*, **150**, A1351 (2003).
8. A. Dobley, J. DiCarlo, and M. K. Abraham, *Proc. 41st Power Sources Conferences*, Philadelphia, PA, P.61 (2004).
9. T. Kuboki, T. Okuyama, T. Ohsaki, and N. Takami, *J. Power Sources*, **146**, 766 (2005).
10. A. Debert, J. Bao, G. Armstrong, and P. G. Bruce, *J. Power Sources*, **174**, 1177 (2007).
11. T. Ogasawara, A. Debart, M. Holfazel, P. Novak, and P. G. Bruce, *J. Am. Chem. Soc.*, **128**, 1390 (2006).
12. A. Debart, A. J. Paterson, J. Bao, and P. G. Bruce, *Angew. Chem. Inter. Ed.*, **47**, 4521 (2008).
13. F. Mizuno, S. Nakanishi, Y. Kotani, S. Yokoishi, and H. Iba, *Electrochemistry*, **78**, 403 (2010).
14. G. Q. Zhang, J. P. Zheng, R. Liang, C. Zhang, B. Wang, M. Au, M. Hendruchson, and E. J. Plichta, *J. Electrochem. Soc.*, **158**, A822 (2011).
15. F. Cheng, J. Shen, B. Peng, Y. Pan, Z. Tao, and J. Chen, *Nature Chemistry*, **3**, 79 (2011).
16. A. K. Thapa, K. Saimen, and T. Ishihara, *Electrochem. Solid-State Lett.*, **13**, A165 (2010).
17. A. K. Thapa and T. Ishihara, *J. Power Sources*, **196**, 7016 (2011).
18. F. Kleitz, S. H. Choi, and R. Ryoo, *Chem. Commun.*, **17**, 2136 (2003).
19. T. W. Kim, F. Klutz, P. Paul, and R. Ryoo, *J. Am. Chem. Soc.*, **127**, 7601 (2005).
20. B. D. McCloskey, D. S. Bethune, R. M. Sheldy, G. Girishkumar, and A. C. Luntz, *J. Phys. Chem. Lett.*, **2**, 1161 (2011).
21. S. A. Freunberger, Y. Chen, Z. Peng, J. M. Griffin, L. J. Hardwick, F. Barde, P. Novak, and P. G. Bruce, *J. Am. Chem. Soc.*, **133**, 8040 (2011).
22. J. Y. Wu, S. H. Chien, and B. Z. Wan, *Ind. Eng. Chem. Res.*, **40**, 94 (2011).
23. H. Kanai, M. Linthuoto, M. Matsumura, and J. B. Moffat, *J. Molecular Catalysis A*, **251**, 181 2006).
24. A. Staykov., T. Kamachi, T. Ishihara, and K. Yoshizawa, *J. Phys. Chem. C*, **112**, 19501 (2008).
25. M. Piccinini, E. N. Ntainjua, J. K. Edwards, A. F. Carley, J. A. Moulijn, and G. J. Hutchings, *Phys. Chem. Chem. Phys.*, **12**, 2488 (2010).
26. K. Honkala and K. Laasonena, *J. Chem. Phys.* **115**, 2297 (2001).
27. C. O. Laoire, S. Mukerjee, K. M. Abraham, E. J. Plichta, and M. A. Hendrickson, *J. Phys. Chem. C.*, **113**, 20127 (2009).
28. C. O. Laoire, S. Mukerjee, K. M. Anraham, E. J. Plichta, and M. A. Hendrickson, *J. Phys. Chem.C.*, **114**, 9178 (2010).